Journal of the Mechanical Behavior of Biomedical Materials 83 (2018) 94–101

Contents lists available at ScienceDirect

Journal of the Mechanical Behavior of Biomedical Materials

journal homepage: www.elsevier.com/locate/jmbbm

Random spectrum fatigue performance of severely plastically deformed titanium for implant dentistry applications

D. Rittel[a,*], K. Shemtov-Yona[a], R. Lapovok[b]

[a] Faculty of Mechanical Engineering, Technion, 32000 Haifa, Israel
[b] Institute for Frontier Materials, Deakin University, Australia

ARTICLE INFO

Keywords:
Severe plastic deformation
Titanium
Dental implants
Random spectrum
Fatigue

ABSTRACT

Severe plastic deformation (SPD) has long been known to confer superior mechanical properties for many metals and alloys. In the general field of biomedical devices, and dental implants in particular, the superior strength of SPD-processed commercially pure (CP) titanium, that may surpass that of the stronger Ti6Al4V alloy, has been associated with a superior fatigue resistance. Such a property would make those materials both biocompatible and strong alternatives to the currently used titanium alloy.

However, the fatigue characterization reported so far in the literature relies on a very small sample size, thereby precluding any meaningful statistical analysis.

This paper reports and compares systematic fatigue testing of various grades as-received and SPD processed Grade 4 CP-Ti using the recently developed random spectrum loading approach, in both air and 0.9% saline solution.

The results of this study do not support the claim that the SPD process, albeit causing noticeable strengthening, confers any advantage to Grade 4 CP-Ti in terms of fatigue response.

1. Introduction

With the discovery of the Hall-Petch relationship (Hall, 1951; Petch, 1953), a substantial research effort has been invested in producing and characterizing the mechanical properties of “small-grained” or simply nanograined materials. The main incentive for this effort is the substantial increase in yield (and flow) strength of ultrafine grained materials, albeit at the expense of their strain hardening capabilities (Jia et al., 2001; Ramesh, 2009; Rittel et al., 2017b), or even their propensity for dynamic shear localization under impact, see. e.g. (Jia et al., 2003; Wei et al., 2004). Yet, the benefits of the grain refinement are not experienced for any grain size, but there exists a limit for which the “inverse Hall-Petch” operates, causing a reduction in strength due to grain boundary sliding as opposed to pure dislocation-mediated plasticity (Mercier et al., 2007; Trelewicz et al., 2008).

The production of nanograined materials involves a “break up” of the metallic grain structure while limiting recrystallization and grain growth phenomena. The most popular method of achieving a very fine grain size consists of the application of very large strains (severe plastic deformation – SPD) using ECAP (equal channel angular pressing), or other well developed techniques (Valiev et al., 2006). ECAP processing involves repeated deformation through the die with two equal intersecting channels. The severe shear strain is introduced in the narrow band along channels intersection without change of the rod geometry. 90° rotation of the sample between passes, known as route B_C, results in e intensified grain fragmentation (Valiev et al., 2006).

Commercially pure (CP) titanium and Ti6Al4V are very often used for the fabrication of prosthetic and dental implants, for their combined strength and biocompatibility (Brunette et al., 2015; Elias et al., 2008). Concerning dental implants specifically, the latter may experience relatively rare mechanical failures due to fatigue that develops with the repeated mastication loads in variable intraoral environment (K Shemtov-Yona and Rittel, 2016a; Shemtov-Yona and Rittel, 2015, 2014). Given the relative variability of the mastication loads, one would naturally seek to develop/use stronger alloys in implant dentistry (Rittel et al., 2017a). Here one must note that, whereas CP Ti is universally recognized as a biocompatible material, the Ti6Al4V alloy has raised concerns regarding the potential toxicity of its alloying elements (Elias et al., 2008; Matusiewicz, 2014).

However, it is also well evidenced that Ti6Al4V is noticeably stronger than CP-Ti, a property that makes the former quite attractive for prosthetic applications.

The fatigue properties of metallic alloys are usually reported in terms of load vs. number of cycles to failure (S/N curve (Suresh, 1998)),

* Corresponding author.
E-mail address: merittel@technion.ac.il (D. Rittel).

https://doi.org/10.1016/j.jmbbm.2018.04.012
Received 26 February 2018; Received in revised form 29 March 2018; Accepted 12 April 2018
Available online 14 April 2018
1751-6161/

noting that the latter may require extensive statistical processing (Nicholas, 2003; Schijve, 2009; Shemtov-Yona and Rittel, 2016b). Without detailed comparative analysis, based on the testing of a large sample size, one cannot draw firmly anchored conclusions regarding ranking of various grades of material. Concerning dental implants, the current standards (ISO, 2016) require a rather small sample size per load level that precludes any statistical analysis.

Several studies have established the fact that severe plastic deformation can significantly increase the yield and flow strength of CP-Ti, bringing those properties close or even superior to those of Ti6Al4V, see e.g. (Elias et al., 2008; Medvedev et al., 2015, 2016a; Mishnaevsky et al., 2014; Valiev et al., 2006).

In parallel, a few studies have compared the fatigue properties of those materials, and come to the conclusion that nanograined CP-Ti has superior fatigue properties when compared to Ti6Al4V (Figueiredo et al., 2014; A. Medvedev et al., 2016b; Medvedev et al., 2015). However, the tested sample size was relatively small (one specimen per load level), so that this conclusion was qualitative and not statistically supported.

In the field of fatigue testing of dental implants, it was recently proposed to address the problem by means of functional testing of the implant. The idea here is that instead of looking for a fatigue limit, one should expose the implant to a random loading spectrum until its final fracture (K Shemtov-Yona and Rittel, 2016b; Shemtov-Yona and Rittel, 20162016c). One of the attracting characteristics of this approach is that each tested group is characterized by its mean longevity with its standard deviation, making the comparison between different tested groups quite straightforward. This comes as an alternative to the S/N curve for which each load level has its mean longevity and standard deviation, together with the complexity that in the finite life regime, the number of cycles to failure is statistically distributed, whereas in the transition regime, the load becomes statistically distributed.

Consequently, this paper compares the fatigue response of SPD CP-Ti with that of as-received Ti6Al4V, using the random spectrum loading approach, for both room-air and saline solution testing.

The paper is organized as follows. We first describe the materials, specimens and briefly the random spectrum procedure. Next we report the results obtained for each batch of tests, followed by a discussion in which the results are statistically compared, ending by a conclusions section.

2. Materials and methods

2.1. Materials

The tested materials consist of undeformed and SPD processed Grade 4 CP-Ti, and as-received Ti6Al4V, (12.7 mm rod). All materials, except for the Ti6Al4V, were kindly provided by Dr. R. Lapovok. Table 1 lists the designation of the materials, noting that the SPD processed materials underwent 4 passes of ECAP at 2 mm/s speed and a variable amount of additional cold work (drawing).

Table 1
The materials tested in this study. Note that 4P360-1 and 2 underwent similar processing but originate from 2 different batches.

Original Marking	Designation	Material	Remarks
Round 12.7	AR	CP Ti	Undeformed-reference
Round 5	4P480	CP Ti	4 passes + drawing, total strain 480%
Al 0017-23	4P360-1	CP Ti	4 passes + drawing, total strain 360%
4 passes	4P360-2	CP Ti	4 passes + drawing, total strain 360%
Ti6Al4V	Ti64	Ti6Al4V	As-received

2.2. Specimens

The specimens used in both static and fatigue tests were cylindrical, 20 mm long with a nominal diameter of 4.85 mm. A square notch was machined at mid-length, 1 mm in width and nominal depth of 0.25 mm. The Appendix section provides details about each tested specimen, including its exact dimensions, as a result of slight variability in the manufacturing process.

2.3. Random spectrum

The random spectrum loading methodology has been described in detail in (K Shemtov-Yona and Rittel, 2016b; Shemtov-Yona and Rittel, 20162016c), and will only be briefly exposed here. The idea is to generate a random loading spectrum that spans from 10 N to 2500 N in this work, generated as a series of loading blocks, with a randomly variable frequency of 1–3 Hz. Some of the blocks are randomly assigned a 0 load value to mimic pauses (relevant for testing in fluid atmosphere). The upper limit is decided upon after quasi-static testing and all the reported results in this work are generated upon application of the same spectrum. The random spectrum approach is described schematically in Appendix 1. Consequently, the outcome of the test is the time to fracture of the specimen, as reported in the Appendix 2 section.

2.4. Loading apparatus and setup

The loading apparatus is an MTS servo-hydraulic machine, driven under load control. The specimen is inserted in a holding block, with the bottom flank of the notch aligned flush with the block, thereby creating the initial stress concentration required to generate a fatigue crack in a controlled location, namely the small square notch. All the specimens are inclined at a 30 degrees angle with respect to the machine crosshead. The configuration used here is identical to that used in all our previous works, see e.g. (Shemtov-Yona and Rittel, 2016a).

Tests were carried out in room air or in 0.9% saline solution, as in (K. Shemtov-Yona and Rittel, 20162016c), but the static tests were only carried out in room air since the saline solution is not expected to influence the mechanical characteristics of the material over short time durations that are characteristic of quasi-static testing.

2.5. Fractographic analysis

All specimens were examined visually. Next, four representative specimens, all made of CP-Ti were selected for fractographic examination using a Quanta 200 scanning electron microscope.

3. Results

3.1. Quasi-static testing in room air

Two specimens of each material were tested, as shown in Table 2.

The results of the quasi-static bending tests clearly indicate 2 kinds of mechanical characteristics: The “soft” material, CP-Ti AR, for which the failure load is inferior to 4000 N, and the remaining “hard” materials, 4P480, 4P360-1 and 2, and Ti6Al4V, for which the failure load clearly exceeds 5000 N. At this stage, we did not carry out additional

Table 2
Quasi-static test results.

Designation	Material	Failure load 1 [N]	Failure load 2 [N]
AR	Gr 4 CP Ti	3836	3873
4P480	Gr 4 CP Ti	5429	5880
4P360-1	Gr 4 CP Ti	5354	5295
4P360-2	Gr 4 CP Ti	5391	5273
Ti64	As-rec. Ti6Al4V	5450	5367

Table 3
Random spectrum loading tests results. The reported numbers indicate the average time to fracture and its standard deviation in seconds. The minimum and maximum values are calculated by subtracting (or adding) the standard deviation to the mean value. Note that the minimum calculated value for the hard-saline test is unphysical.

Group	Test	Average [s]	SD [s]	Min [s]	Max [s]
Hard	Air	22,206	15,647	6558	37,853
Soft	Air	18,176	10,398	7779	28,574
Hard	Saline	9652	11,078	−1426	20,730
Soft	Saline	6820	3522	3299	10,342
Ti6Al4V	Air	30,787	22,437	8350	53,224
Ti6Al4V	Saline	24,369	12,892	11,477	37,261

tests to try and discriminate between the soft and hard groups, so that the results reported in the sequel will consider the grouped materials according to their hard/soft denomination, while the Ti6Al4V will be considered separately for comparison purposes.

Table 4
Percentage of macroscopically flat and slant fracture surfaces.

Group	Atmosphere	# Specimens	% Flat	% Slant
Hard	Air	9	33	67
Hard	Saline	9	44	56
Soft	Air	7	100	0
Soft	Saline	5	0	100
Ti6Al4V	Air	8	75	25
Ti6Al4V	Saline	8	100	0

3.2. Random spectrum testing

Table 3 lists the average time to fracture and the standard deviation for dry and wet tests per material group.

The detailed results for each specimen are reported in the Appendix section. As expected from any fatigue test (random or cyclic), the results exhibit a large scatter, so that statistical analysis is needed, as reported

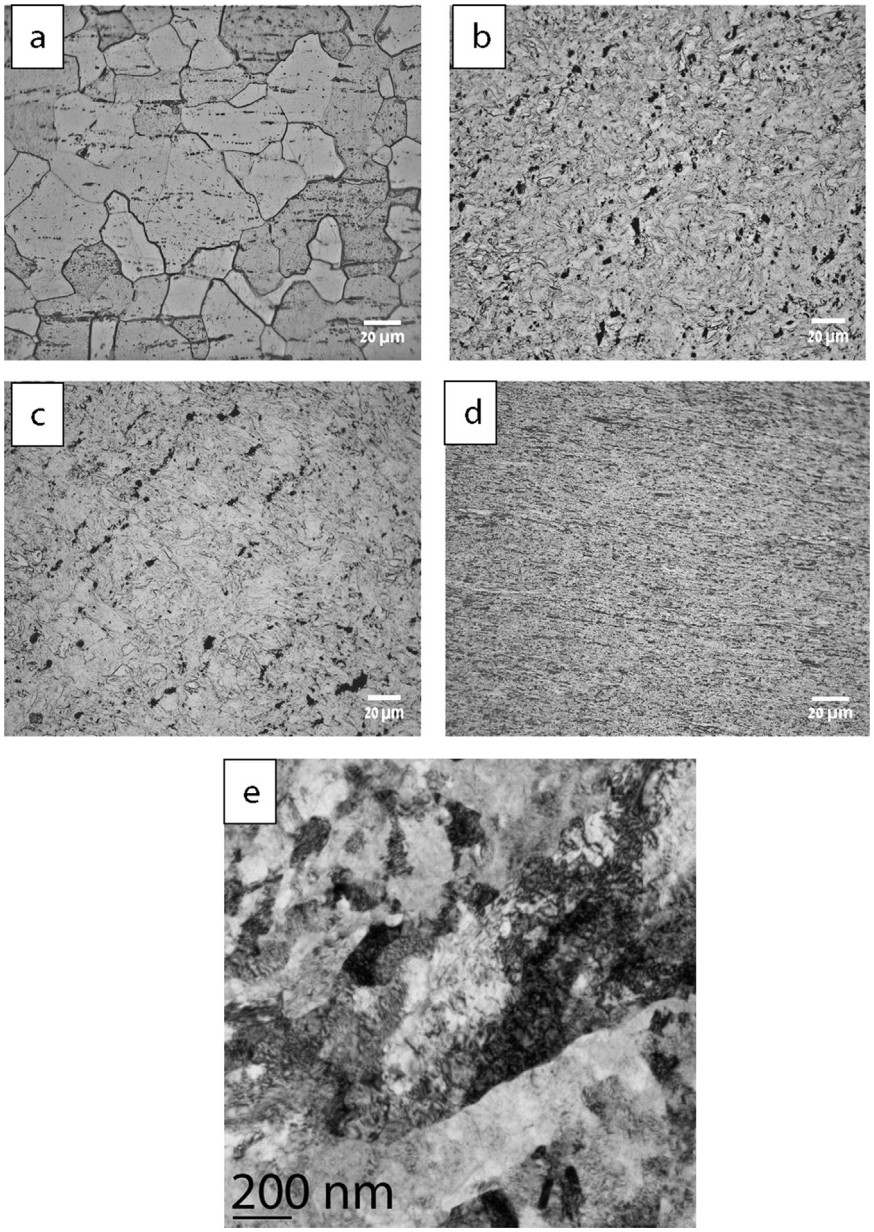

Fig. 1. Typical microstructure (longitudinal) of (a) undeformed AR, (b) 4P360-1, (c) 4P360-2, and (d) 4P-480 grades. Kroll's etchant, optical metallography. (e) TEM BF image of a specimen prepared from a longitudinal section of the 4P-480 batch (courtesy A. Medvedev).

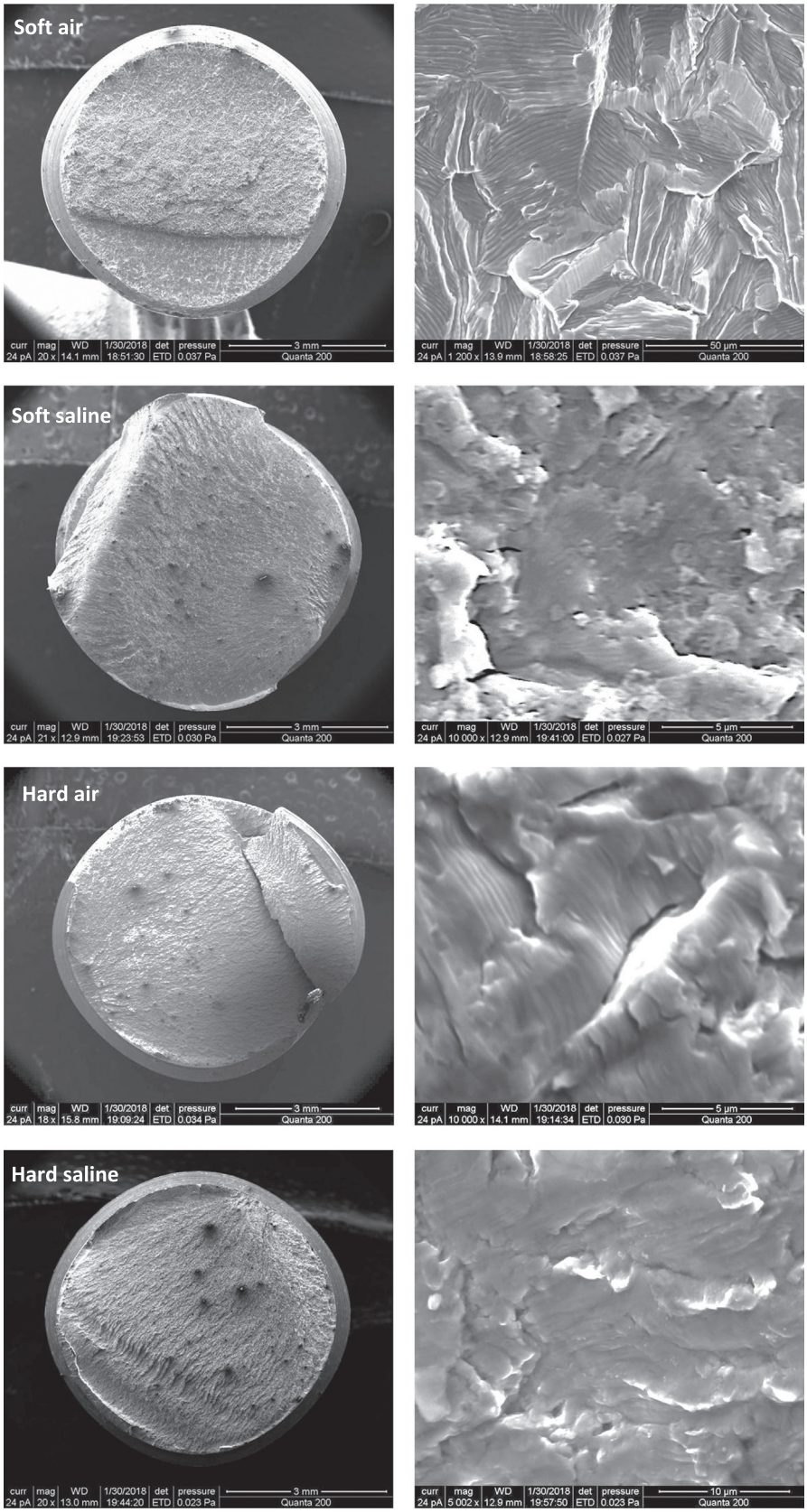

Fig. 2. Typical scanning electron fractographs of hard and soft fractured specimens in air and in saline solution.

in the Discussion section.

3.3. Optical microstructural characterization

The microstructure of representative specimens of the CP-Ti grades of is shown in Fig. 1, for specimens extracted in the longitudinal direction.

The reference material, as-received CP-Ti, is characterized by relatively equiaxed grains with a representative diameter of 10–20 μm. The grains are clearly delineated by their boundaries, as opposed to those of the other severely deformed materials. In particular, the 4P-480 exhibits some sort of fibrous microstructure for which individual grains are not discernible by OM. Consequently, a specimen was prepared for transmission electron microscopy, as shown in Fig. 1e. This examination reveals a non-uniform grain size, namely fine grains with a diameter of 50–100 nm and coarse grains with a diameter of about 1 μm. This non-uniform structure is believed to be a result of high ECAP processing speed. It was shown by contrast that microstructure in samples ECAP processed at 0.2 mm/s is uniform and consists of ultrafine grains within 100–200 nm range (Medvedev et al., 2015).

3.4. Fractographic analysis

Macroscopic examination of the broken specimens revealed two different classes of fracture surfaces: flat and slant, as listed in Table 4.

Four specimens were randomly selected for scanning electron fractographic examination, with the time to fracture in seconds indicated in parentheses:

R2 - soft-air (5105 s), SP3 - hard air (19954 s), W129 – soft saline (8784 s), and W231 – hard saline (3444 s). representative fracture surface topographies are shown in Fig. 2.

4. Discussion

The mechanical characteristics of the tested materials reveal two “classes” of CP-Ti, namely the original “weak” and the SPD processed “strong grades. Those are compared with the commonly used Ti6Al4V alloy for which SPD-CP Ti could act as a replacement material. The following discussion addresses the main results of this study.

All the specimens were tested in room air and in saline solution under random spectrum loading. Here, it is worth noting that the maximum spectral load (2500 N) represents approximately 65% (2500/3800 N) of the soft class’ strength, versus 45% (2500/5500 N) of the strong class’ strength. Yet, all the specimens were tested with the same exact spectrum.

At that stage, it is interesting to look at the results of paired t-tests that were carried out on all pairs of materials, as shown in Table 5, in which we retain only those groups that are statistically different from the others.

The differences outlined in Table 5 can be summarized as follows, considering also the average lifetimes of each group listed in Table 3:

- Soft air (18,176) vs. soft saline (6820)
- Hard air (22,206) vs. hard saline (9652)
- Hard air (22,206) vs. soft saline (6820)
- Ti64 air (30,787) vs. soft saline (6820)
- Ti64 air (30,787) vs. hard saline (9652)
- Ti64 saline (24,369) vs. soft saline (6820)
- Ti64 saline (24,369) vs. hard saline (9652)

The results indicate that the base (soft) and hard SPD CP-Ti's lifetime is shortened by the saline solution. However, no difference is observed for both hard and soft batches tested in air or saline, respectively. Ti6Al4V shows no statistical difference when compared with hard or soft air tests. However, when Ti6Al4V is tested in saline solution, it clearly outperforms both the hard and the soft grades.

Table 5
p values for t-tests of pairs of materials. The table lists only statistically significant different batches.

	Soft air	Soft saline	Hard air	Hard saline	Ti64 air	Ti64 saline
Soft air		0.0349				
Soft saline	0.0349		0.0403		0.0214	0.0066
Hard air		0.0403		0.053		
Hard saline			0.053		0.0156	0.0135
Ti64 air		0.0214		0.0156		
Ti64 saline		0.0066		0.0135		

With that, one should notice that regarding Ti6Al4V, our previous results (Shemtov-Yona and Rittel, 2016b) clearly indicated that the saline solution reduces the spectrum loading life of the material. One possible reason could be that, whereas the peak load of the previous spectrum tests was 1000 N, representing 88% of the implants strength (Shemtov-Yona and Rittel, 2016b), the peak load of the currents tests did not exceed 45% of the specimens’ strength. Since the saline solution is likely to activate a stress corrosion mechanism, the difference in the applied peak load (stress) level is likely to influence the rate of saline-induced damage formation.

The scanning electron fractographic analysis reveals, as expected, the presence of fatigue striations on the fracture surface of the specimens. However, the initial fatigue cracks are generally short, which makes their identification more difficult. As a general observation, the fatigue striations in all the ECAP processed specimens are faint and thus hard to discern. For all the investigated grades, testing in saline solution makes the fatigue striations even fainter. Consequently, future failure analyses of SPD processed titanium implants may be more delicate to perform, all the more so if an aggressive solution like the present saline is involved.

On a more general note, one might have expected that the stronger the material, the more resistant it is to fatigue. However, this is not the case. One possible reason can be the lack of microstructural homogeneity in terms of grain size and morphology that was revealed by the TEM examination. This point deserves further investigation.

5. Conclusions

- The results of the current study definitely confirm the well-established fact that severe plastic deformation of commercially pure titanium brings its strength of the latter to a level that compares with that of commercial Ti6Al4V.
- However, when random spectrum fatigue life is considered, the SPD processed Grade 4 CP-Ti does not possess any advantage in terms of longevity to fracture with respect to the base CP-Ti, for both air and saline solution testing. This result seems to contradict previous claims about the superior fatigue properties of SPD titanium, at least in room air.
- When compared with Ti6Al4V, the hard material performs like the SPD processed one in room air.
- However, when tested in a saline solution, the SPD Ti exhibits inferior fatigue properties with respect to Ti6Al4V.
- The present study does not support the claim that SPD Ti, despite its superior strength, offers any advantage compared to Ti6Al4V when random spectrum fatigue is considered.

Acknowledgements

Mr. A. Reuven is kindly acknowledged for his technical assistance. Dr. A.E. Medvedev is acknowledged for providing the TEM characterization of the SPD processed material.

Appendix 1. Random spectrum loading

see: Fig. A1

The essence of the method is summarized graphically below. A specimen, in this case cylindrical with a notch is loaded at a 30 degree angle using a conventional servohydraulic testing machine. The loading consists of a succession of random loads, whose maximum value here is 1200 N, applied at a variable frequency between 0 and 3 Hz. Some pauses are inserted randomly to mimic pauses occurring during the service of dental implants, and such pauses become especially relevant when the tests are carried out in an atmosphere other than air. The outcome of the tests is the time elapsed until specimen fracture. Consequently, a group of N specimens is represented by a single value of the average time to failure with its standard deviation. This is to be contrasted with a conventional fatigue tests (e.g. S/N) for which each load level is identified with an average time to failure and standard deviation.

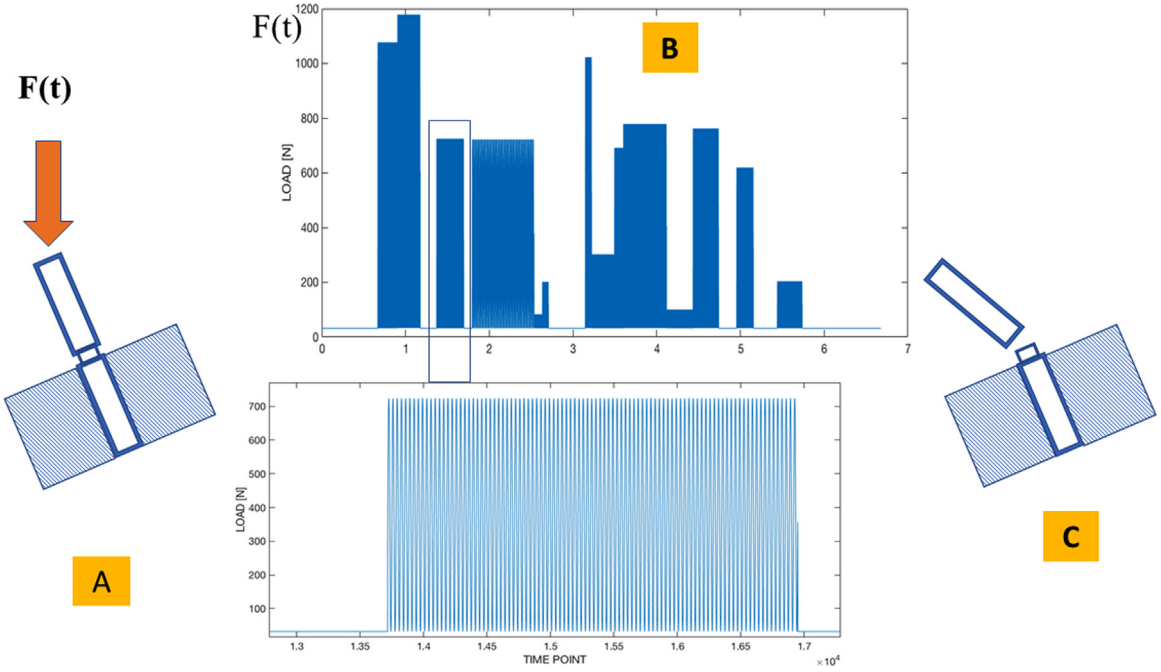

Fig. A1. (A) A notched cylindrical specimen is loaded by a succession of random loads at random frequencies (B). The specimen finally breaks (C) and the fracture time is measured.

Appendix 2. Results of the random spectrum loading tests for each group (time to fracture in [s])

SOFT-AIR	Specimen	Diameter	Notch	Time
AR	R1	4.81	4.23	**9090**
AR	R2	4.76	4.52	**5105**
AR	R3	5.19	4.31	**7515**
AR	R5	4.83	4.29	**17,541**
AR	R6	4.85	4.24	**28,974**
AR	R7	4.88	4.31	**29,833**
AR	R8	4.85	4.26	**29,854**
AR	R9	4.85	4.29	**17,498**
SOFT-SALINE	**Specimen**	**Diameter**	**Notch**	**Time**
AR	W123	4.83	4.36	**8997**
AR	W124	4.84	4.27	**10,660**
AR	W125	4.83	4.25	**10,392**
AR	W126	4.83	4.28	**4286**
AR	W127	4.84	4.36	**9119**
AR	W129	4.84	4.32	**8784**
AR	W1210	4.86	4.35	**8773**
HARD-AIR	**Specimen**	**Diameter**	**Notch**	**Time**
4P360-2	4p3	4.85	4.30	**19,594**
4P360-2	4p6	4.83	4.21	**25,485**
4P360-2	4p7	4.79	4.16	**29,799**

4P360-2	4p8	4.86	4.27	**17,326**
4P360-2	4p9	4.77	4.30	**9083**
4P360-2	4p10	4.84	4.31	**25,358**
4P360-2	4p11	4.88	4.30	**60,857**
4P360-1	232	4.86	4.29	**9509**
4P360-1	233	4.86	4.30	**6211**
4P360-1	234	4.87	4.31	**18,833**
HARD-SALINE	**Specimen**	**Diameter**	**Notch**	**Time**
4P360-1	W231	4.85	4.30	**3444**
4P360-1	W232	4.84	4.33	**4265**
4P360-1	W233	4.85	4.29	**2225**
4P360-1	W234	4.85	4.29	**2729**
4P360-1	W235	4.83	4.29	**2972**
4P480	WR51	4.84	4.36	**9012**
4P480	WR52	4.84	4.34	**5093**
4P480	WR53	4.82	4.36	**6921**
4P480	WR54	4.86	4.44	**34,309**
4P480	WR55	4.87	4.42	**25,546**
Ti6Al4V-AIR	**Specimen**	**Diameter**	**Notch**	**tTime**
Ti64	642	4.81	4.29	**28,976**
Ti64	643	4.83	4.23	**11,969**
Ti64	644	4.82	4.24	**43,628**
Ti64	645	4.77	4.29	**32,871**
Ti64	648	4.9	4.33	**29,600**
Ti64	649	4.9	4.28	**86,959**
Ti64	651	4.86	4.32	**7780**
Ti64	653	4.82	4.28	**16,781**
Ti64	654	4.85	4.34	**29,491**
Ti64	655	4.84	4.29	**19,814**
Ti6Al4V-SALINE	**Specimen**	**Diameter**	**Notch**	**Time**
Ti64	W642	4.88	4.32	**43,643**
Ti64	W643	4.87	4.4	**28,350**
Ti64	W647	4.86	4.38	**16,314**
Ti64	W648	4.87	4.51	**33,587**
Ti64	W649	4.83	4.36	**12,260**
Ti64	W651	4.88	4.39	**17,187**
Ti64	W652	4.88	4.33	**17,950**
Ti64	W653	4.88	4.37	**10,657**
Ti64	W654	4.89	4.39	**46,340**
Ti64	W655	4.89	4.32	**17,403**

References

Brunette, D.M., Tengvall, P., Textor, M., Thomsen, P., 2015. Titan. Med. http://dx.doi.org/10.1017/CBO9781107415324.004.

Elias, C.N., Lima, J.H.C., Valiev, R., Meyers, M. a., 2008. Biomedical applications of titanium and its alloys. J. Miner. Met. Mater. Soc. 46–49. http://dx.doi.org/10.1007/s11837-008-0031-1.

Figueiredo, R.B., Eduardo, E.R., Zhao, X., Yang, X., Liu, X., Cetlin, P.R., Langdon, T.G., 2014. Improving the fatigue behavior of dental implants through processing commercial purity titanium by equal-channel angular pressing. Mater. Sci. Eng. A 619, 312–318. http://dx.doi.org/10.1016/j.msea.2014.09.099.

Hall, E.O., 1951. The deformation and ageing of mild steel: III discussion of results. Proc. Phys. Soc. Lond. 64, 747–753.

ISO, 2016. ISO 14801:2016(en), Dentistry — Implants — Dynamic Loading Test for Endosseous Dental Implants.

Jia, D., Ramesh, K.T., Ma, E., 2003. Effects of Nanocrystalline and Ultrafine Grain Sizes on Constitutive Behavior And Shear Bands in Iron, 51, pp. 3495–3509. <https://doi.org/10.1016/S1359-6454(03)00169-1>.

Jia, D., Wang, Y.M., Ramesh, K.T., Ma, E., Zhu, Y.T., Valiev, R.Z., 2001. Deformation behavior and plastic instabilities of ultrafine-grained titanium. Appl. Phys. Lett. 79, 611–613.

Matusiewicz, H., 2014. Potential release of in vivo trace metals from metallic medical implants in the human body: from ions to nanoparticles – A systematic analytical review. Acta Biomater. 10, 2379–2403. http://dx.doi.org/10.1016/j.actbio.2014.02.027.

Medvedev, A., Ng, H.P., Lapovok, R., Estrin, Y., Lowe, T.C., Anumalasetty, V.N., 2015. Comparison of laboratory-scale and industrial-scale equal channel angular pressing of commercial purity titanium. Mater. Lett. 145, 308–311. http://dx.doi.org/10.1016/j.matlet.2015.01.051.

Medvedev, A.E., Lapovok, R., Estrin, Y., Lowe, T.C., Anumalasetty, V.N., 2016a. Bending fatigue testing of commercial purity titanium for dental implants. Adv. Eng. Mater. http://dx.doi.org/10.1002/adem.201600002.

Medvedev, A.E., Ng, H.P., Lapovok, R., Estrin, Y., Lowe, T.C., Anumalasetty, V.N., 2016b. Effect of bulk microstructure of commercially pure titanium on surface characteristics and fatigue properties after surface modification by sand blasting and acid-etching. J. Mech. Behav. Biomed. Mater. 57, 55–68. http://dx.doi.org/10.1016/j.jmbbm.2015.11.035.

Mercier, S., Molinari, A., Estrin, Y., 2007. Grain size dependence of strength of nanocrystalline materials as exemplified by copper: an elastic-viscoplastic modelling approach. J. Mater. Sci. 42, 1455–1465.

Mishnaevsky, L., Levashov, E., Valiev, R.Z., Segurado, J., Sabirov, I., Enikeev, N., Prokoshkin, S., Solov'Yov, A.V., Korotitskiy, A., Gutmanas, E., Gotman, I., Rabkin, E., Psakh'E, S., Dluhoš, L., Seefeldt, M., Smolin, A., 2014. Nanostructured titanium-based materials for medical implants: modeling and development. Mater. Sci. Eng. R Rep. 81, 1–19. http://dx.doi.org/10.1016/j.mser.2014.04.002.

Nicholas, T., 2003. Recent Advances in High Cycle Fatigue, Defense Technical Information Center.

Petch, N.J., 1953. The cleavage strength of polycrystals. J. Iron Steel Inst. 25–28 (London).

Ramesh, K.T., 2009. Nanomaterials - Mechanics and Mechanisms, Nanomaterials - Mechanics and Mechanisms. Springer, New York. http://dx.doi.org/10.1007/978-0-387-09783-1_6.

Rittel, D., Shemtov-Yona, K., Korabi, R., 2017a. Eng. Dent. Implants. http://dx.doi.org/10.1007/s40496-017-0148-9.

Rittel, D., Zhang, L.H.H., Osovski, S., 2017b. Mechanical characterization of impact-induced dynamically recrystallized nanophase. Phys. Rev. Appl. 44012, 1–7. http://dx.doi.org/10.1103/PhysRevApplied.7.044012.

Schijve, J., 2009. Fatigue of structures and materials. Fatigue Struct. Mater. 25, 1–622. http://dx.doi.org/10.1007/978-1-4020-6808-9.

Shemtov-Yona, K., Rittel, D., 2016a. Fatigue of dental implants: facts and fallacies. Dent. J. 4, 16. http://dx.doi.org/10.3390/dj4020016.

Shemtov-Yona, K., Rittel, D., 2016b. Random spectrum loading of dental implants: an alternative approach to functional performance assessment. J. Mech. Behav. Biomed. Mater. 62, 1–9. http://dx.doi.org/10.1016/j.jmbbm.2016.04.030.

Shemtov-Yona, K., Rittel, D., 2016c. Fatigue failure of dental implants in simulated intraoral media. J. Mech. Behav. Biomed. Mater. 62, 636–644. http://dx.doi.org/10.1016/j.jmbbm.2016.05.028.

Shemtov-Yona, K., Rittel, D., 2015. On the mechanical integrity of retrieved dental implants. J. Mech. Behav. Biomed. Mater. 49, 290–299. http://dx.doi.org/10.1016/j.jmbbm.2015.05.014.

Shemtov-Yona, K., Rittel, D., 2014. Identification of failure mechanisms in retrieved fractured dental implants. Eng. Fail. Anal. 38, 58–65. http://dx.doi.org/10.1016/j.engfailanal.2014.01.002.

Suresh, S., 1998. Fatigue of Materials. Cambridge University Press.

Trelewicz, J.R., Schuh, C.A., Schuch, C.A., 2008. the Hall-Petch breakdown at high strain rates: optimizing nanocrystalline grain size for impact applications. Appl. Phys. Lett. 93, 171916. http://dx.doi.org/10.1063/1.3000655.

Valiev, R.Z., Estrin, Y., Horita, Z., Langdon, T.G., Zehetbauer, M.J., Zhu, Y.T., 2006. Producing bulk ultrafine grained materials by severe plastic deformation. JOM 58, 33–39. http://dx.doi.org/10.1007/s11837-006-0213-7.

Wei, Q., Kecskes, L., Jiao, T., Hartwig, K.T., Ramesh, K.T., Ma, E., 2004. Adiabatic shear banding in ultrafine-grained Fe processed by severe plastic deformation. Acta Mater. 52, 1859–1869. http://dx.doi.org/10.1016/j.actamat.2003.12.025.